Structural Behavior of Highly Concentrated Hyaluronan

Paolo Matteini,*,†,‡ Luigi Dei,§ Emiliano Carretti,§ Nicola Volpi,⊥ Andrea Goti,‡ and Roberto Pini†

Institute of Applied Physics "Nello Carrara", National Research Council, via Madonna del Piano 10, I-50019 Florence, Italy, Department of Chemistry and CSGI Consortium, University of Florence, via della Lastruccia 3, I-50019 Florence, Italy, Department of Animal Biology, Biological Chemistry Section, University of Modena and Reggio Emilia, via Campi 213/D, I-41100 Modena, Italy, and Department of Organic Chemistry "Ugo Schiff", University of Florence, via della Lastruccia 13, I-50019 Florence, Italy

Received January 27, 2009; Revised Manuscript Received March 11, 2009

When investigated under high concentration conditions, hyaluronan (HA) solutions in physiological saline are shown to generate stable superstructures. An abrupt change in the rheological properties observed on increasing the temperature suggests the breaking of certain cooperative bonds. The thermal disruption of the HA superstructure is accompanied by a sharp transition from a long- to a restricted-connectivity water structuring, which is interpreted as a concurrent transition from a stable to a temporary polymer network. The intermolecular associations are considered to be originated by hydrophobic interactions between the nonpolar groups of the polymer backbones.

Introduction

Hyaluronan (HA) is a high molecular mass linear glycosaminoglycan consisting of *N*-acetyl-D-glucosamine (GlcNAc) and D-glucuronic acid (GlcA), which form the disaccharide repeating unit (GlcNAc-β1,4-GlcA-β1,3; Figure 1). HA is a major component of the extracellular matrix of vertebrates, where it is involved in maintaining osmotic balance and reducing friction in tissues such as the synovium, vitreous humor, and cartilage. The distinctive biomechanical properties of HA have been utilized in the development of numerous biomedical products. For example, HA solutions are used as protectants of the cornea in dry eyes, as substitutes for vitreous fluid in eye surgery, and as lubricants in the treatment of osteoarthritic joints. HA also forms the structural basis of the pericellular matrix and contributes to mediating and modulating cell adhesion, as well as other biological processes, such as development, tumor metastasis, and inflammation.[1−3]

HA's wide range of biological functions suggests the existence of a correspondingly large repertoire of conformations. Extensive research has been carried out over the past sixty years on the structural properties expressed by HA in solution; at present, however, the question is still controversial. In dilute solutions at physiological pH and ionic strength, HA chains assume a stiffened, random worm-like coil configuration with a persistence length of about 5−7 nm, which occupies a large hydrodynamic volume.[3,4] The local stiffening responsible for generating the persistence length is partly due to the mutual electrostatic repulsion among carboxylate groups and mainly to the existence of intramolecular hydrogen bonds that bridge adjacent monosaccharide units, which restricts rotation and flexion at the glycosidic linkages.[5−7] Molecular dynamics simulations and NMR data on HA oligosaccharides in water have suggested that these hydrogen bonds are in rapid (in the subnanosecond time scale) exchange with water.[8,9] The resulting picture is a highly dynamic ensemble of chaotically interchanging semiordered states, as recently confirmed by NMR data.[10,11] Because of the huge hydrodynamic volume and high molecular weight of HA, its individual chains are brought into contact and begin to entangle with each other at concentrations above ~1 mg/mL (for MW about 1−2 MDa).[5,12] This leads to high elastoviscous solutions showing nonideal behavior (non-Newtonian viscosity), which, however, can be predicted by a simple expression for polymer solution viscosity, not invoking stable associations.[3] Experimental results of HA diffusion in a wide range (0.05−10 mg/mL) of concentrations also confirmed that the overlapping of the domains of the individual molecules does not lead to the formation of stable networks, typical of a gel.[13]

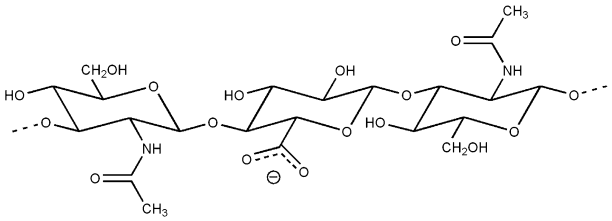

Figure 1. Schematic representation of a trisaccharide of HA that includes the repeating disaccharide unit consisting of *N*-acetyl-D-glucosamine and D-glucuronic acid.

However, evidence of HA aggregation has also been reported: short HA segments have been demonstrated to self-associate in physiological solution,[14,15] while a variety of intermolecular aggregates were observed when HA was spread on surfaces.[16,17] Furthermore, on the basis of electron microscopy[18] and NMR[19] data, Scott and co-workers proposed the formation of highly ordered arrangements mediated by hydrogen-bonding and hydrophobic interactions among antiparallel HA chains. These chain−chain interactions were reported to be reversibly disaggregated by an increase in temperature or by alkalinization.[18,20] Recent infrared spectroscopy studies have suggested the formation of three-dimensional superstructures of HA chains stabilized by water bridges.[21−23] This water-mediated supramolecular

* To whom correspondence should be addressed. E-mail: p.matteini@ifac.cnr.it.
† Institute of Applied Physics of the National Research Council.
‡ Department of Organic Chemistry, University of Florence.
§ Department of Chemistry and CSGI Consortium, University of Florence.
⊥ Department of Animal Biology, University of Modena and Reggio Emilia.

10.1021/bm900108z CCC: $40.75
Published on Web 04/09/2009

assembly was shown to break down progressively when the temperature was increased to over ~40 °C,[24] in accordance with previous NMR observations.[20]

In the present work we aim to investigate more thoroughly the ability of HA to form supramolecular aggregates. Previous studies have mainly focused the attention on dilute solutions of HA to study its physiochemical properties without the influence of nonspecific interactions. However, highly concentrated HA can be found in some biological compartments, as in the synovium or in the umbilical cord. Moreover, pericellular, intercellular, and intracellular sites, where HA performs several critical biological roles,[25,26] are characterized by high levels of macromolecular crowding. These constraining environments can potentially lead to intermolecular associations by favoring the approach between adjacent chains, and thus to increasing the "effective" molecular concentration, as suggested by a recently proposed concept.[27,28] We used a combination of different methodologies (falling ball (FB) method, rheology, differential scanning calorimetry (DSC), Fourier transform infrared (FTIR) spectroscopy, and polarized-light microscopy (PLM)) to build up a consistent picture of HA's ability to assemble stable superstructures under high concentration conditions.

Experimental Section

Materials. We used HA obtained from a bacterial source to minimize the protein-mediated aggregation of polymer chains that might have occurred if HA from an animal source had been employed.[12,29] In particular, HA sodium salt from *Streptococcus equi* (Esperis S.p.A., Milan, Italy) that had a molecular mass of approximately 1.000 kDa was used. By means of specific quantitative spectrophotometric analysis, the protein content was found to be lower than ~0.025%. Different concentrations of the polymer (in the 10−100 mg/mL range) in 0.15 M NaCl solution were separately prepared in small glass vials. The samples were treated accordingly to previous procedures reported in the literature,[30,31] that is, homogenizing by mechanically mixing and then heating in a thermostat oven at ~60 °C. The time of heating (ca. 4 h) was selected to avoid any type of molecular weight reduction, as previously reported.[32] After cooling and leaving the samples to rest until complete elimination of possible bubbles formed during preparation, the samples were subjected to the various measurements.

Falling Ball Method. A tungsten carbide ball with a diameter of 0.5 mm and density of 14.9 g/mL was put at the top of a glass tube 10 cm in length and 1 cm in diameter previously filled with the HA sample. The distance covered by the ball in a fixed time at a constant temperature was measured. The reported parameter was the mean velocity (v/mms^{-1}) of the ball falling down the tube: depending on its value the fixed time was adjusted from 1 to 5 min. The glass tube was maintained at constant temperature (±0.1 °C) by means of a thermostatic water bath.

Rheology. The viscosity of the concentrated sample (100 mg/mL) was measured by a Paar Physica UDS200 instrument working in the controlled shear-stress mode. The geometry selected for the measurements was the cone−plate one (2.5 cm diameter, 2° angle). The temperature was maintained constant (±0.1 °C) by means of a Peltier. An aliquot of an equilibrated sample was introduced into the gap with a spatula. At each temperature the viscosity η versus shear rate curve was collected in the 15−60 °C range. The η-value plotted against $1/T$ (K^{-1}) was that deduced from the plateau of the above-mentioned curves in the low shear rate regime.

Differential Scanning Calorimetry. DSC measurements were performed using a Q1000 (TA Instruments) equipped with a universal Analysis 2000 version 3.7A software. Steel sample pans (TA Instruments) hermetically sealed to avoid water evaporation were used. The weight of the samples was checked at the beginning and at the end of the measurements, and only measurements in which no evaporation had occurred were considered. The sample was first equilibrated at 0 °C, heated to 80 °C (first run), cooled down to 0 °C, and then heated again to 80 °C (second run) at a 5 °C min^{-1} rate in both the heating and the cooling mode. Measurements were made under a dry nitrogen flow of 40 cm^3/min. Calibration of the DSC apparatus was performed through the melting of indium.

Infrared Spectroscopy. FTIR spectra were collected in the mid-IR range (4000−1000 cm^{-1}) with a Nexus 870-FTIR (Thermo-Nicolet), in transmittance mode, with a resolution of 4 cm^{-1}, with 32 scans per spectrum, and no mathematical correction (e.g., smoothing) was performed. In a typical experiment, a small amount (about 1.5 mg) of the sample was placed between two CaF_2 windows, which were then sealed using Teflon tape. This was done to avoid possible water evaporation during the recording of spectra at higher temperatures. The spectrum of the CaF_2 probe alone was used as a reference in the absorbance calculations. Curve-fitting of the spectra was performed using the Gaussian deconvolution algorithm of the Peak Fit software (v 4.00, Jandel Scientific, Corde, Madera, CA).

Polarized-Light Microscopy. HA samples were observed under circular polarization, using a polarized-light microscope (Leica DM 2500 P). Typically, a sample amount of about 3 mg was sandwiched between a microscope slide and a glass coverslip, both appropriately pretreated, stored at room temperature for up to one week, and then observed. The purpose of the pretreatment of the glass slides was to create a hydrophilic or a hydrophobic environment. For the former condition, the glasses were first cleaned with a nonionic detergent, treated with a saturated solution of NaOH in ethyl alcohol for 1 h, and then rinsed with water. To generate a hydrophobic environment, the remaining glasses were sprayed with a plasticizer (Plastivel, Mark Service), which, upon drying, formed a thin, transparent, and homogeneous layer over the glass surface.

Results and Discussion

The properties of HA have been investigated in the literature using a variety of techniques, typically in dilute solution, that is, in the 0.1−1 mg/mL range. Under physiological solvent conditions at low concentration, HA molecules adopt a stiffened random coil configuration. By increasing the concentration, because of the extended hydrodynamic domains of the polymer, HA chains begin to entangle conferring to the solution distinctive hydrodynamic properties (the viscoelasticity is dramatically increased).[3] Previous studies on HA at this concentration regime have provided no evidence of strong chain−chain associations, but rather an entanglement coupling behavior that is typical of a temporary polymer network.[13,33] However, HA has been shown to form aggregates in highly crowded biological environments, such as when it is confined in intercellular[34] or intracellular[25] spaces. The aim of this paper was thus to elucidate how the structural features of HA could be affected when studied under high concentration conditions in vitro, which would have great significance for the understanding of biological phenomena occurring in in vivo constricted environments.

Falling Ball. Figure 2 shows a selection of representative results of the FB experiment performed on HA samples. We recall that the axial coordinates reported in Figure 2 (mean velocity (v) of the falling ball vs temperature) are usually employed to evaluate the gelation temperature.[31,35] We used the parameter v to empirically investigate the rheological behavior of our samples with the aim of comparing different concentrations of HA. Results obtained from up to 50 mg/mL-concentrated samples displayed a nearly monotonic increase in v upon an increase in the temperature, which indirectly suggests a monotonic change in the rheological characteristics of these samples. At higher concentration values, a more abrupt change in v was detected. For example, when considering the 100 mg/mL sample, we observed that the solution started to soften at

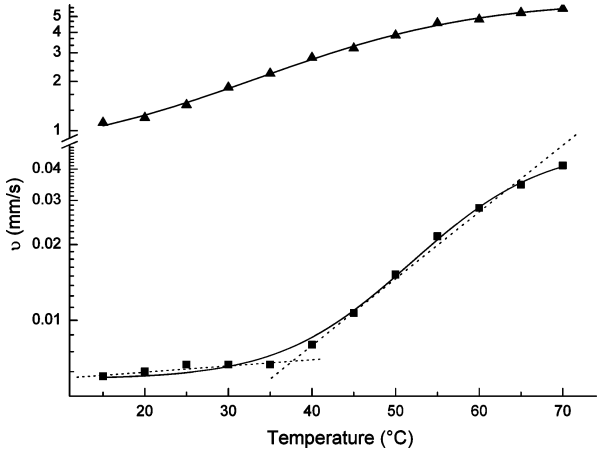

Figure 2. Mean velocity (v; log scale) of a 0.5 mm tungsten carbide ball inside a 100 mg/mL (squares) or a 10 mg/mL (triangles) HA solution in physiological saline as a function of the temperature.

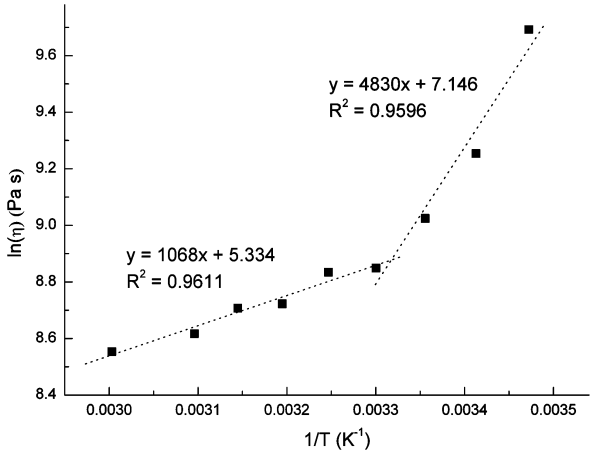

Figure 3. Trend of the ln(viscosity) of a 100 mg/mL HA solution in physiological saline as a function of 1/*T*.

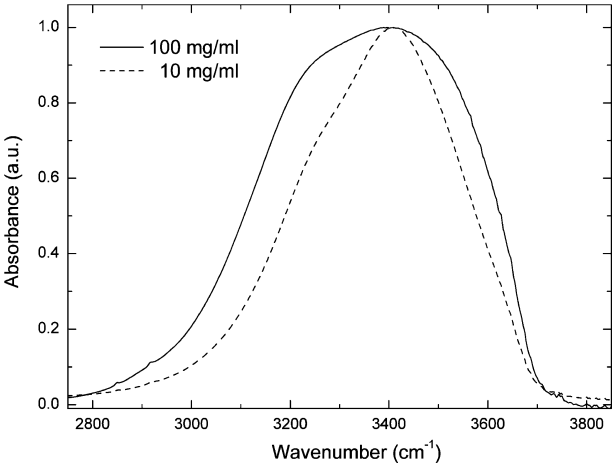

Figure 4. OH stretching band of 10 and 100 mg/mL HA solutions in physiological saline at 20 °C.

~35 °C and became fluid at ~50 °C. The distinct change in the slope of the v observed during the heating of these HA samples could be referred to a loosening of certain cooperative interactions, which are typically found to play a key role in polymer−polymer complexes of polysaccharide systems.[36] Extrapolated lines of the travel distance below and beyond these values furnished a gel-like to fluid-like transition at 35−40 °C, in accordance with previous studies which had ascribed it to a destabilization of a postulated HA supramolecular assembly.[5,24] It is important to underline that the FB method is not reliable for high viscosity systems, because when the fluidity drops down to very low values, the v-parameter is not well detectable. This is the reason why the mean velocity of the falling ball for the 100 mg/mL sample remained almost constant in the 15−35 °C against the predictable viscosity decrease according to the well-known exponential behavior. Indeed, we expected that for the 100 mg/mL sample the viscosity decreased even in the range 15−35 °C, and v should increase too, but probably remaining in a range of η-values too high to determine an appreciable increase of the falling ball velocity. Therefore, to achieve more accurate information on the rheological behavior of the concentrated solution, we carried out viscosity measurements by means of a rheometer.

Rheology. Figure 3 shows the trend of the ln(η) as a function of 1/T in the 15−60 °C temperature range for the 100 mg/mL sample. Two different linear regimes can be noted: the first one occurring between 15 and 30 °C (straight line on the right) and the second one from 30 to 60 °C (straight line on the left). These measurements clarified that the viscosity decreased even at low temperatures, which underlines the scarce reliability of the FB method when the viscosity is very high (see Figure 2 and the previous discussion). It is interesting to notice that there was an abrupt change of the slope at ~30 °C according to what empirically obtained by the FB method. Being the slope of the straight lines associated to the constant of the exponential decay of η versus 1/T (Arrhenius-type behavior), the data shown in Figure 3 indicated a drastic change in the trend of viscosity as a function of temperature at ~30 °C. Therefore, the slope of the straight lines reported in Figure 3 could be interpreted as an empirical parameter for the activation energy associated to the fluid's flow. Our results show that the activation energy decreased abruptly at ~30 °C. This is in accordance with the rupture of supramolecular structures stable up to ~30 °C due to cooperative interactions that start to strongly weaken at this temperature. If this picture is correct, we expect that even the water structuring within the system is affected by the break of this supramolecular assembly: this is the reason why we carried out the analysis of the water structure by means of a spectroscopic technique, namely the infrared spectroscopy, which is reported in the next section.

FTIR. Infrared spectroscopy is a powerful tool for obtaining structural information on the behavior of water molecules embedded in macromolecules, and, thus, in gaining indirect insight into the structure of the latter. The infrared spectrum of HA water solutions was dominated by the broadband relative to the OH stretching of H_2O molecules falling within the 3000−3700 cm^{-1} region (See Figure 4), in accordance with previous observations.[21−23] Considerable differences in the shape of this band were evident from the comparison of the spectra obtained for HA solutions at different concentrations, which unequivocally indicated the presence of different structural water environments.

A first interesting outcome was given by the modulation of the peak intensity of the OH-stretching band as a function of the temperature (Figure 5). The less-concentrated samples showed a nearly monotonic decrement in intensity that could be ascribed to a progressive thinning of the HA film held between the CaF_2 windows, which was caused by a monotonic change in the fluidity of the HA solution, as previously

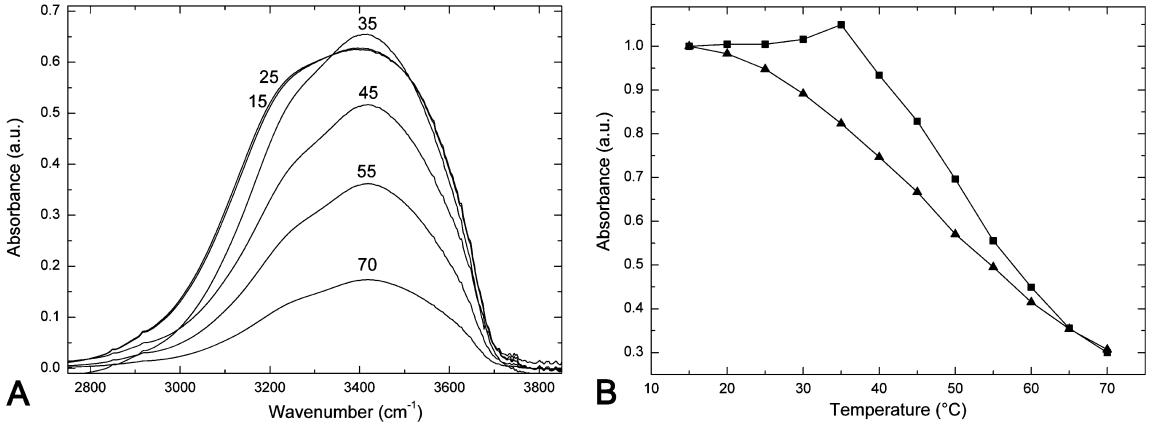

Figure 5. (A) OH stretching band of 100 mg/mL HA in physiological saline at increasing temperatures. (B) Variation in the peak intensity of the OH stretching band as a function of the temperature. Squares: 100 mg/mL; triangles: 10 mg/mL.

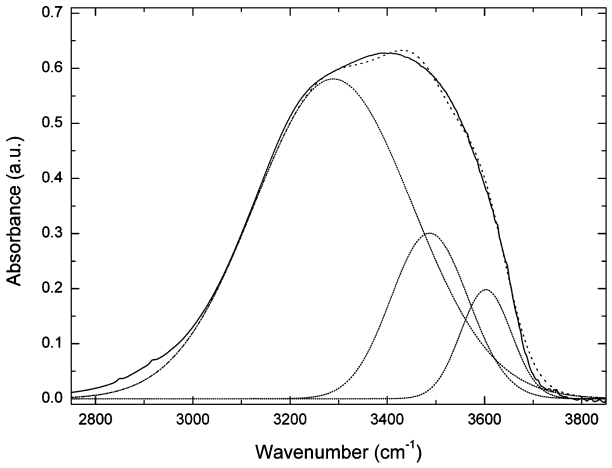

Figure 6. Gaussian deconvolution of the OH band of 100 mg/mL HA in physiological saline at 20 °C.

suggested by the FB measurements (compare Figure 5B with Figure 2, triangles). On the contrary, we observed a sharp change of slope that occurred at ∼35 °C for the more concentrated samples (see Figure 5B, squares). Indeed, from 15 to 35 °C thinning was greatly inhibited, probably due to the very high viscosity of the system in this range of temperature (see Figure 3 and relative discussion). At ∼35 °C, the thinning was no longer inhibited and started to affect the absorbance of the peak (see Figure 5A), resulting in a constant decreasing trend in the 35−70 °C temperature range. Thus, in this case, we could infer the presence of an HA superstructure that undergoes a transition beyond a characteristic temperature threshold, as already suggested by the FB and the rheology measurements.

To qualitatively assess the changes in the OH stretching band arising from an increase in temperature and a variation in concentration, we fitted each spectrum as a sum of three Gaussian curves, in accordance with previous studies.[37−39] An example of fitting is reported in Figure 6. Each of the Gaussian curves accounts for different water populations associated with a particular type of hydrogen bond, as extensively discussed in the literature.[37−42] These are "network water (NW)" molecules, "intermediate water (IW)" molecules, and "multimer water (MW)" molecules. The first type, NW, which is assigned to the lower energy Gaussian curve (∼3300 cm^{-1}), is assumed to be originated from water molecules involved in transient networks that break and form continuously. These water molecules are most likely to be connected tetrahedrally, almost as in ice, thus generating instantaneous H-bonded low-density pathways that extend over a supramolecular level. The second type of water molecules, IW (centered at ca. 3480 cm^{-1}) is ascribed to molecules connected in some way to other water molecules, although unable to develop fully connected patches, and thus, having distorted H-bonds. This water component has an average degree of connection larger than that of dimers or trimers but lower than those participating in the percolating networks. The third kind of water molecules, MW (higher energy Gaussian at ∼3600 cm^{-1}), corresponds to water molecules poorly connected with their environment and standing as free monomers or as dimers or trimers. The latter assignment is supported by the fact that, frequency wise, these MW molecules are close to those found in the vapor phase, just as the NW Gaussian is positioned at a frequency close to that of the OH band in ice.

As water is represented by three different states in the systems (NW, IW, MW), it is reasonable to assume that the total peak area corresponding to the water band is the sum of the peak areas of the different states of water. Thus, we can calculate the fraction of NW, IW, and MW weighted on the total amount of water, and we can plot the variation of the ratio between the area of each Gaussian component (A_i) to the total peak area (A_{tot}) as a function of the temperature.

The A_i/A_{tot} calculated trends relative to these solutions (Figure 7A,B) unveiled a different behavior, mainly of the NW and the IW fractions, as a function of either concentration or temperature. Major modifications were observed for the most concentrated samples examined. For example, if we consider the 100 mg/mL HA solution, "network water" passed from 0.75 up to 25 °C to 0.55 beyond 60 °C, while the "intermediate water" varied from 0.20 to 0.40 in precisely the opposite manner. Thus, a modification of the water structuring occurred when a certain temperature value, that is, 25 °C, was reached; then, after a gradual decrease (for NW) or increase (for IW) between 25 and 60 °C, a constant trend was maintained despite further heating. Instead, less concentrated HA samples (e.g., 10 and 30 mg/mL) showed slight variations in the NW and IW fractions upon heating, which were mainly centered at around 0.70 and 0.25, respectively. Interestingly, the 100 mg/mL HA sample showed initial (up to 25 °C) A_i/A_{tot} values of NW and IW that were more similar to those found typically for the 10 mg/mL sample than for the 30 mg/mL sample.

Semidiluted HA solutions have previously been shown to form temporary networks, whose average mesh size was predicted to be progressively lower than 20 nm for solutions

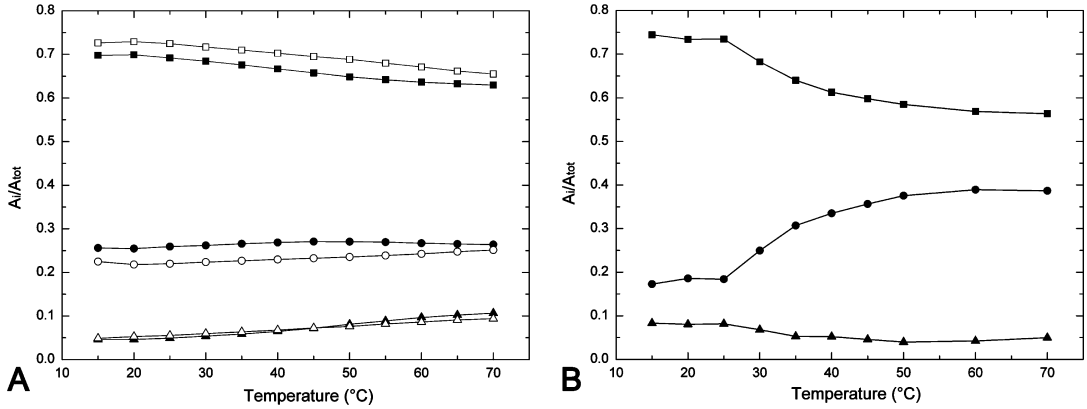

Figure 7. Ratio of the area of the *i*th Gaussian component (A_i) to the total peak area (A_{tot}) vs temperature. (A) NW (square), IW (circles), and MW (triangles) fractions of 10 mg/mL (open) and 30 mg/mL (filled) HA in physiological saline. (B) NW (square), IW (circles), and MW (triangles) fractions of 100 mg/mL HA in physiological saline.

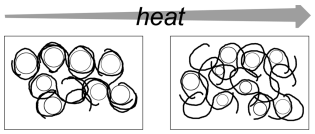

Figure 8. Proposed scheme of HA network rearrangement (from stable to temporary) during heating.

progressively more concentrated than 10 mg/mL.[43,44] The confinement of water inside low-sized pores can be disadvantageous for long-distance water connectivities, while favoring the more restricted connectivities, as previously reported for water confined in fluorocarbon reverse micelles.[38] Accordingly, in our measurements, the 30 mg/mL HA sample showed NW and IW values that were, respectively, lower and higher, on average, as compared with the 10 mg/mL solution, suggesting a moderate effect of confinement. The plot of the 100 mg/mL HA sample revealed a different trend. First, it unequivocally showed a transition between two different kinds of water structuring and, thus, of HA. At low temperatures, that is, below 25 °C, NW was favored possibly because of stable associations among HA chains. This made possible the formation of a large-pore-size polymer network (see the scheme proposed in Figure 8), which favored the formation of long-distance connectivities of water molecules with respect to small-sized water aggregates. These pores should have a dimension comparable to that of the 10 mg/mL sample, if we consider the similarity of their initial NW values. Beyond 25 °C, the intermolecular interactions were supposed to break progressively, leading to a polydisperse entanglement that, on average, was more crowded than that of less concentrated solutions, because of the higher local chain density. In fact, we observed a considerable decrease in NW and, simultaneously, an increase in IW, which are both well in agreement with our hypothesis.

FTIR results pointed out the formation of stable supramolecular assemblies only at the highest concentrations considered. The sharp change in shape of the OH stretching band starting at 25 °C, indicating a transition from a large- to a restricted-connectivity water structuring, suggested a concurrent transition from a stable to a temporary HA network. Furthermore, it should be noted that the low-temperature threshold supposed to disrupt the network is well in agreement with the occurrence of weak intermolecular associations among the HA chains.

DSC. DSC analysis of highly concentrated HA solutions was performed to obtain a quantitative estimate of the structural transition showed by FB, rheology, and FTIR measurements.

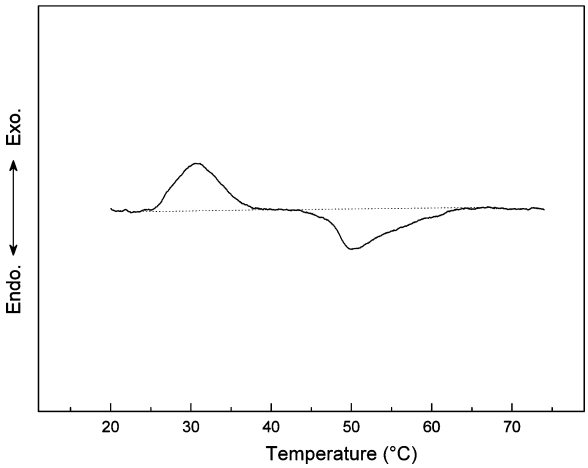

Figure 9. DSC curve (second run measurement) of 100 mg/mL HA in physiological saline recorded at a 5 °C/min scanning rate.

Figure 9 shows a heating curve relative to the 100 mg/mL HA sample acquired at a 5 °C/min scanning rate. The DSC curve enables the detection of an exothermic and an endothermic transition at 25−35 °C and at 45−60 °C, respectively. The latter was ascribed to a gel-like to fluid-like transition. In fact, the onset of this transition is well in agreement with the threshold values characterizing the sharp change in the rheological properties of concentrated HA samples, which were reported above (see Figures 2, 3, and 5b, squares). The exothermic transition starting at 25 °C is not easy to interpret: it may derive from a transient reorganization of the HA chains stimulated by a rather low temperature regime. Moreover, it appears to be an essential part of the process that leads to the disruption of the HA supramolecular network, since it matches the starting temperature of water restructuring found by the FTIR measurements (see Figure 7b). The measured enthalpies calculated from the area of the two peaks were on the order of 100−200 cal/mol (as referred to the repeating disaccharide unit). These values are compatible with weak noncovalent interactions like those characteristic of van der Waals and hydrophobic forces, which are frequently responsible for the structuring of polysaccharide systems.[36]

PLM. This technique can selectively visualize the birefringence originating from anisotropic structures, which are seen as shining bodies on a dark background. The analyzed samples consisted of thin films of HA solutions in physiologic saline, obtained by sandwiching a small amount of the sample between

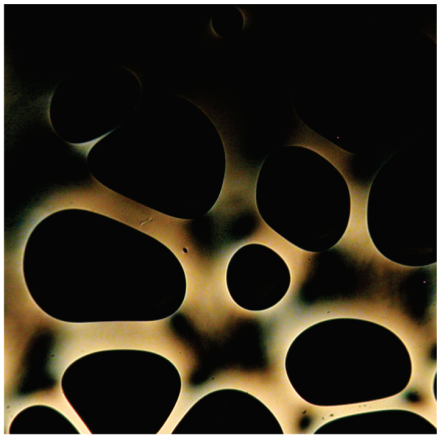

Figure 10. PLM image of an HA sample (100 mg/mL) in physiological saline sandwiched between polar microscope slides, after 1 week of storage at room temperature.

a microscope slide and a coverslip, both previously pretreated. The pretreatment of the microscope glass slides consisted of creating either a hydrophilic or a hydrophobic environment, as previously detailed in Experimental Section.

Soon after the preparations, all types of films appeared homogeneously dark. This indicated a lack of extensive ordered chain-assemblies over the concentration scale examined. During a week of storage at room temperature, following a slight loss of water due to evaporation, the HA deposits on polar glass tended to lose their initial shape and to assume ragged edges consisting of honeycomb-like structures (Figure 10). In these locations, the HA strands were probably induced to approach one another, creating a bright and persistent birefringence. On the other hand, HA films deposited within plasticized slides (hydrophobic substrate) were slightly reduced in size, but preserved their linear edges and lacked any type of birefringence. Similar results were found for all the differently concentrated samples considered (in the 10−100 mg/mL range), even if the greater the concentration was, the less the time was required for the development of the birefringence textures (within the hydrophilic environment).

The HA molecule owns hydrophobic groups oriented above and below the average plane of each sugar ring, whereas the hydrophilic groups are displayed around the perimeter of the rings, thus creating relatively hydrophobic and hydrophilic faces, respectively.[19] The existence of such a 2-fold character can account for the different behavior observed when changing the environment from polar to hydrophobic. HA placed in between hydrophilic surfaces appeared to be prone to generating ordered assemblies. This is understandable if we consider that HA keeps its hydrophilic faces in contact with the polar surfaces while using its hydrophobic patches to mediate the assembly with the other polymer chains. This observation can be explained thermodynamically by an entropically driven process due to water molecules initially bound to the polymer and then freed by the association of approaching polymer segments,[3] which is even more favored during water loss process. The observed local ordered assemblies can thus be interpreted as the result of the generation of favorable interactions among the HA chains, probably induced by a hydrophobic effect. On the other hand, the lack of birefringence observed in the HA samples sandwiched between plasticized surfaces can be interpreted in accordance with a moderate affinity for this environment, ascribable to the nonpolar groups of the polymer. The preferential interaction of the hydrophobic patches with the plasticized substrate probably inhibited the possibility of employing them for generating extended ordered assemblies. Similar results have been recently obtained by Cowman and co-workers by means of atomic force microscopy.[45] They showed that HA deposited on mica (hydrophilic) tended frequently to generate intermolecular associations, differently from when a graphite substrate (hydrophobic) was used.

In comparison with aged HA films spread on a polar glass, HA in concentrated solutions is expected to generate looser networks mediated by restricted junction zones (which are replaced by dynamic entanglements under a lower concentration regime). Under certain perturbing conditions, such as those carried out in this experiment, these junction zones are encouraged to develop into more extended and stiffened intermolecular associations, which were actually detected by our PLM imaging. With this assumption, we can ascribe to hydrophobic interactions also the self-associations operating in stable HA networks in solutions, which, in addition, agree with the low enthalpy values obtained from the DSC analysis.

Conclusions

The multifaceted analysis that we carried out enabled us to bring to light the ability of HA solutions in physiological saline to generate stable superstructures under high concentration conditions. FB and FTIR measurements of the less concentrated HA samples suggested the presence of a temporary polymer network, in which the overlapping of individual HA domains did not lead to stable interactions. By increasing the concentration, the crowded local environment was assumed to promote the intermolecular association of HA chains. FB, rheology and FTIR analyses of highly concentrated HA solutions revealed the presence of stable polymer networks that dissolved upon heating. DSC pointed out the existence of a gel-like to fluid-like transition, while it excluded any involvement of strong intermolecular interactions. PLM suggested that chain−chain associations were driven by hydrophobic interactions, and this is essentially compatible with the low enthalpy values obtained from the DSC analysis. Therefore, we can hypothesize a switching from temporary to stable HA networks as a function of concentration. The latter probably originated from the formation of junction zones mediated by hydrophobic interactions.

It is interesting to notice that FTIR data indicate the lowest temperature value for the transition, which is in good agreement with the measured property. Indeed, the other techniques (FB, rheology, DSC, PLM) investigate bulk properties, which become sensitive to the rupture of the supramolecular assembly when the process starts to involve large domains, that occurs with a certain temperature delay. This phenomenon is particularly enhanced when using DSC that is the only technique with a scan rate (5 °C/min). On the other hand, FTIR starts to detect the break of the supramolecular assembly before, because it "sees" the water restructuring at the beginning of the nucleation of the rupture process; in this context, the small exothermic peak detected by DSC at low temperature could be ascribed to some polymer hydration changes somehow associated to the loosening of cooperative interactions among the polymer chains. Further studies, for example by means of NMR relaxation analysis, could get more detailed information about the proposed mechanism.

In physiological compartments, the presence of a large number of macromolecules makes the space highly crowded. In practice, this leads to an enhancement of the "effective"

concentration of the individual macromolecules.[27] The intermolecular associations of highly concentrated HA solutions can be viewed as a strategy of the system to reduce its free energy by maximizing the available volume (and minimizing the excluded volume), as is normally observed in living systems.[28] It can be speculated that this process is possibly more favored in the presence of physiological concentrations of Na^+, which can actually induce a shielding of the electrostatic repulsion between the anionic groups of the HA chains.[17] On the basis of the results presented here, we would like to emphasize the importance of taking into account the "effective" macromolecular concentration in the context of future studies dealing with the structuring of HA and of other glycosaminoglycans in physiological conditions. Furthermore, at this concentration the biological activity of the polymer could be partially altered, which is actually an issue that is usually disregarded in the case of more diluted solutions.

Acknowledgment. We are very grateful to Drs. Francesca Ridi and Azzurra Macherelli for their assistance in performing DSC measurements. L.D. and E.C. thank the Consorzio Interuniversitario per lo Sviluppo dei Sistemi a Grande Interfase, the Ministero dell'Università e della Ricerca Scientifica (PRIN 2007−2008), and Università degli Studi di Firenze (Fondi d'Ateneo ex-60%) for financial support.

References and Notes

(1) Lapcík, L. J.; Lapcík, L.; De Smedt, S.; Demeester, J.; Chabrecek, P. *Chem. Rev.* **1998**, *98*, 2663–2684.
(2) Day, A. J.; Sheehan, J. K. *Curr. Opin. Struct. Biol.* **2001**, *11*, 617–622.
(3) Cowman, M. K.; Matsuoka, S. *Carbohydr. Res.* **2005**, *340*, 791–809.
(4) Hayashi, K.; Tsutsumi, K.; Nakajima, F.; Norisuye, T.; Teramoto, A. *Macromolecules* **1995**, *28*, 3824–3830.
(5) Morris, E. R.; Rees, D. A.; Welsh, E. J. *J. Mol. Biol.* **1980**, *138*, 383–400.
(6) Scott, J. E.; Heatley, F.; Moorcroft, D.; Olavesen, A. H. *Biochem. J.* **1981**, *199*, 829–832.
(7) Almond, A.; Sheehan, J. K.; Brass, A. *Glycobiology* **1997**, *7*, 597–604.
(8) Almond, A.; Brass, A.; Sheehan, J. K. *Glycobiology* **1998**, *8*, 973–980.
(9) Almond, A.; Brass, A.; Sheehan, J. K. *J. Phys. Chem. B* **2000**, *104*, 5634–5640.
(10) Cowman, M. K.; Feder-Davis, J.; Hittner, D. M. *Macromolecules* **2001**, *34*, 110–115.
(11) Almond, A.; Deangelis, P. L.; Blundell, C. D. *J. Mol. Biol.* **2006**, *358*, 1256–1269.
(12) Fouissac, E.; Milas, M.; Rinaudo, M. *Macromolecules* **1993**, *26*, 6945–6951.
(13) Gribbon, P.; Heng, B. C.; Hardingham, T. E. *Biophys. J.* **1999**, *77*, 2210–2216.
(14) Turner, R. E.; Lin, P. Y.; Cowman, M. K. *Arch. Biochem. Biophys.* **1988**, *265*, 484–495.
(15) Cowman, M. K.; Liu, J.; Li, M.; Hittner, D. M.; Kim, J. S. In *The Chemistry, Biology, and Medical Applications of Hyaluronan and Its Derivatives*; Laurent, T. C., Ed.; Portland Press: London, 1998; pp 17−24.
(16) Cowman, M. K.; Li, M.; Balazs, E. A. *Biophys. J.* **1998**, *75*, 2030–2037.
(17) Cowman, M. K.; Spagnoli, C.; Kudasheva, D.; Li, M.; Dyal, A.; Kanai, S.; Balazs, E. A. *Biophys. J.* **2005**, *88*, 590–602.
(18) Scott, J. E.; Cummings, C.; Brass, A.; Chen, Y. *Biochem. J.* **1991**, *274*, 699–705.
(19) Scott, J. E.; Heatley, F. *Proc. Natl. Acad. Sci. U.S.A.* **1999**, *96*, 4850–4855.
(20) Scott, J. E.; Heatley, F. *Biomacromolecules* **2002**, *3*, 547–553.
(21) Haxaire, K.; Maréchal, Y.; Milas, M.; Rinaudo, M. *Biopolymers* **2003**, *72*, 10–20.
(22) Haxaire, K.; Maréchal, Y.; Milas, M.; Rinaudo, M. *Biopolymers* **2003**, *72*, 149–161.
(23) Maréchal, Y.; Milas, M.; Rinaudo, M. *Biopolymers* **2003**, *72*, 162–173.
(24) Giannotti, M. I.; Rinaudo, M.; Vancso, G. J. *Biomacromolecules* **2007**, *8*, 2648–2652.
(25) Evanko, S. P.; Parks, W. T.; Wight, T. N. *J. Histochem. Cytochem.* **2004**, *52*, 1525–1535.
(26) Evanko, S. P.; Tammi, M. I.; Tammi, R. H.; Wight, T. N. *Adv. Drug Delivery Rev.* **2007**, *59*, 1351–1365.
(27) Rivas, G.; Ferrone, F.; Herzfeld, J. *EMBO Rep.* **2004**, *5*, 23–27.
(28) Minton, A. P. *J. Biol. Chem.* **2001**, *276*, 10577–10580.
(29) Krause, W. E.; Bellomo, E. G.; Colby, R. H. *Biomacromolecules* **2001**, *2*, 65–69.
(30) Takahashi, M.; Hatakeyama, T.; Hatakeyama, H. *Carbohydr. Polym.* **2000**, *41*, 91–95.
(31) Fujiwara, J.; Takahashi, M.; Hatakeyama, T.; Hatakeyama, H. *Polym. Int.* **2000**, *49*, 1604–1608.
(32) Min, B. H.; Lee, J. Y.; Moon, T. S.; Cho, K. Y.; Kim, J. H. In *Hyaluronan, structure, metabolism, biological activities, therapeutic applications*; Balazs, E. A., Hascall, V. C., Eds.; Matrix Biology Institute: Edgewater, NJ, 2005; Vol. 1, pp 55−59.
(33) Blundell, C. D.; Deangelis, P. L.; Almond, A. *Biochem. J.* **2006**, *396*, 487–498.
(34) Scott, J. E.; Thomlinson, A. M.; Prehm, P. *Exp. Cell. Res.* **2003**, *285*, 1–8.
(35) Chung, Y. M.; Simmons, K. L.; Gutowska, A.; Jeong, B. *Biomacromolecules* **2002**, *3*, 511–516.
(36) Rinaudo, M. *Macromol. Biosci.* **2006**, *6*, 590–610.
(37) Onori, G.; Santucci, A. *J. Phys. Chem.* **1993**, *97*, 5430–5434.
(38) Brubach, J.-B.; Mermet, A.; Filabozzi, A.; Gerschel, A.; Lairez, D.; Krafft, M. P.; Roy, P. *J. Phys. Chem. B* **2001**, *105*, 430–435.
(39) Dei, L.; Grassi, S. *J. Phys. Chem. B* **2006**, *110*, 12191–12197.
(40) Boissier, C.; Brubach, J.-B.; Mermet, A.; de Marzi, G.; Bourgaux, C.; Prouzet, E.; Roy, P. *J. Phys. Chem. B* **2002**, *106*, 1032–1035.
(41) Temsamani, M. B.; Maeck, M.; El Hassani, I.; Hurwitz, H. D. *J. Phys. Chem. B* **1998**, *102*, 3335–3340.
(42) Lasagabaster, A.; Abad, M. J.; Barral, L.; Ares, A. *Eur. Polym. J.* **2006**, *42*, 3121–3132.
(43) De Smedt, S. C.; Lauwers, A.; Demeester, J.; Engelborghs, Y.; De Mey, G.; Du, M. *Macromolecules* **1994**, *27*, 141–146.
(44) Hardingham, T. E. In *Hyaluronan, structure, metabolism, biological activities, therapeutic applications*; Balazs, E. A., Hascall, V. C., Eds.; Matrix Biology Institute: Edgewater, NJ, 2005; Vol. 1, pp 67−76.
(45) Spagnoli, C.; Korniakov, A.; Ulman, A.; Balazs, E. A.; Lyubchenko, Y. L.; Cowman, M. K. *Carbohydr. Res.* **2003**, *340*, 929–941.

BM900108Z